Resonance Search

Unblinding Preparedness

C. Bravo, K. McCarty, R. Paremuzyan

Introduction

- The resonance search is performed on 10% of the 2016 data.
- The final invariant mass distribution, after all vertex selection cuts are applied, is shown.

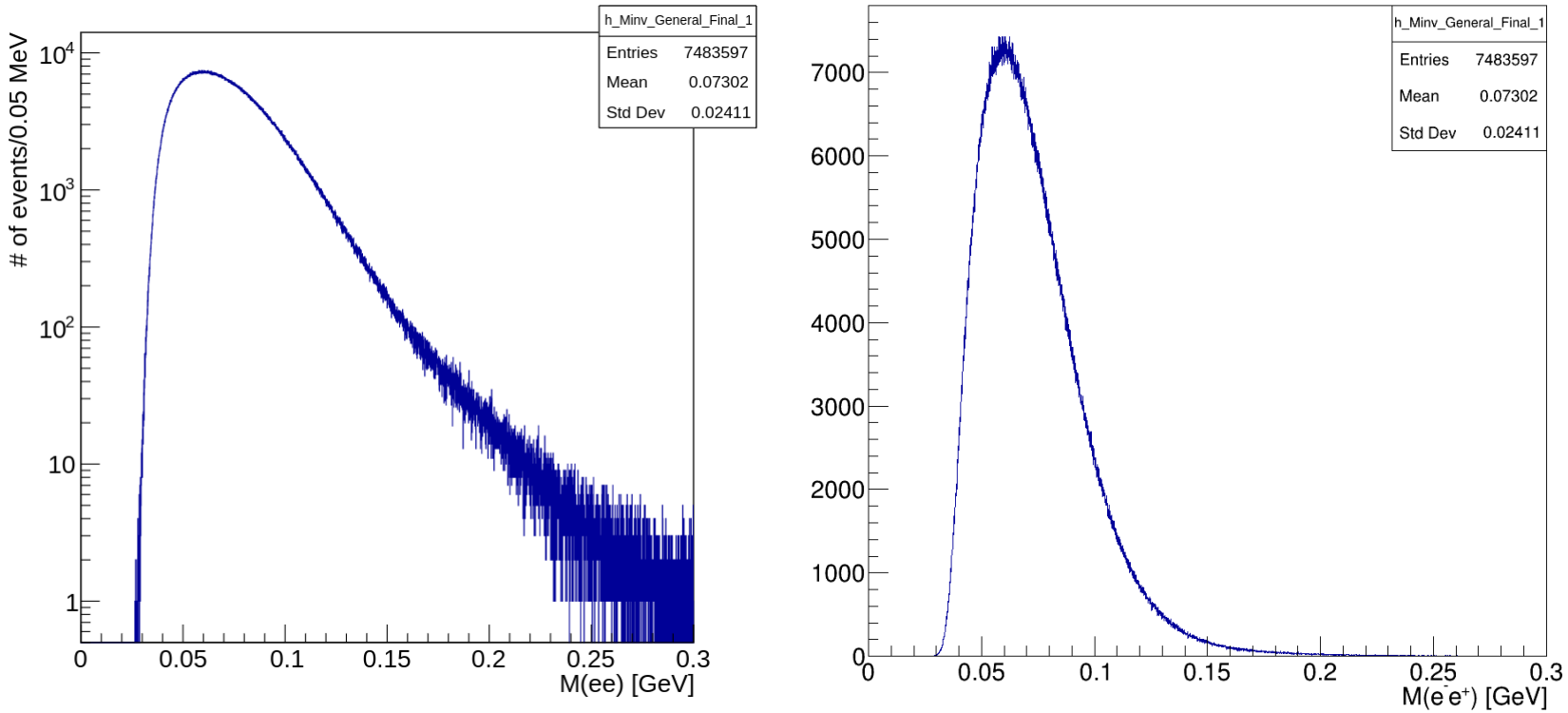

- The selection cuts are not discussed, as they have been covered previously.

Part I: Mass Resolution

Mass Resolution

- Understanding the mass resolution is key part of the analysis.
  - Monte Carlo can provide both the momentum and mass resolution, but it is imperative that they be validated against experimental data.
- The mass resolution of the A' within the ε region of interest is expected to be several orders of magnitude smaller than the mass resolution of HPS, so the width of an observed signal should represent the detector mass resolution itself.
- In data, the Møller process ($e^-e^- \rightarrow e^-e^-$) may be employed to find the mass resolution for a single mass point.
  - e^+e^- decays (such as the case for an A') have similar properties with regard to multiple scattering and electromagnetic showers, and this are expected to have similar mass resolutions at the same mass.
  - The center of mass energy for an e^-e^- is fixed for a given beam energy.

$$M(e^-e^-) = \sqrt{S_{cm}} = \sqrt{2m_{e^-}^2 + 2E_{beam}m_{e^-}} \approx \sqrt{2E_{beam}m_{e^-}} = 48.498\ \text{MeV}$$

Møller Event Selection

- The “MOUSE” cuts for Møller events are employed as a first pass filter.
  - An electron pair, with particles in opposite halves of the calorimeter.
  - $0.8 \cdot E_{beam} < p_{sum} < 1.2 \cdot E_{beam}$

- Next, more stringent cuts are applied.

- Using stringent cuts is not a problem!
  - For determining the mass resolution, the *purity* of the sample is important, not the cross-section.

Møller Fiducial Cuts

- Fiducial cuts are defined for Møller events, depicted as the regions outlined in black lines.

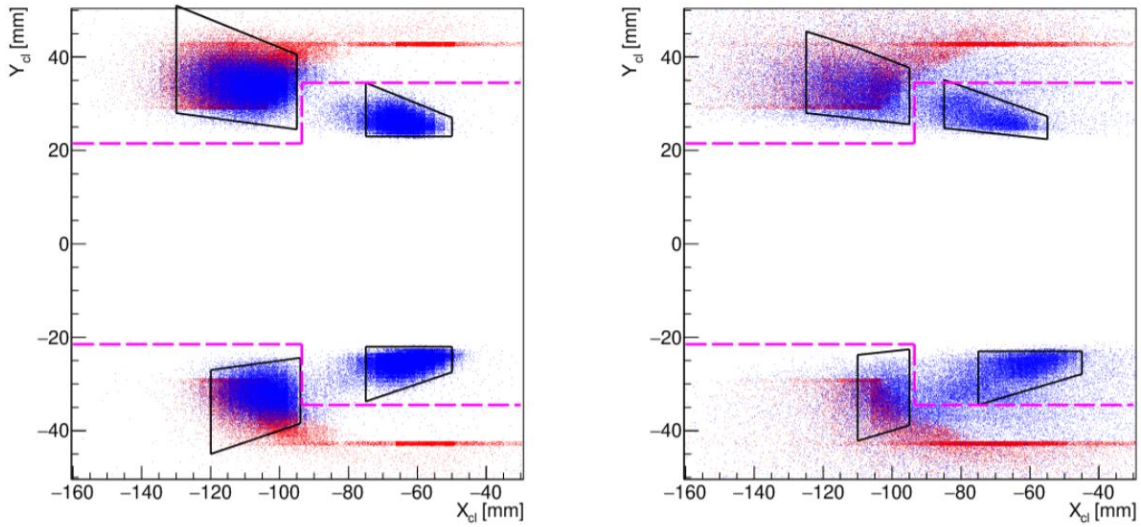

- Fiducial cuts are different for Monte Carlo versus data, possibly due to differences in detector geometry. (Swapping doesn't change the results.)
- There is a gap between the two regions. This is because sometimes both Møller electrons pass through the beam hole, and no trigger occurs.

Møller Timing and Momentum Sum Cuts

- Cuts are defined for both the time difference between two tracks and the sum of their momenta.

Time Difference

Monte Carlo

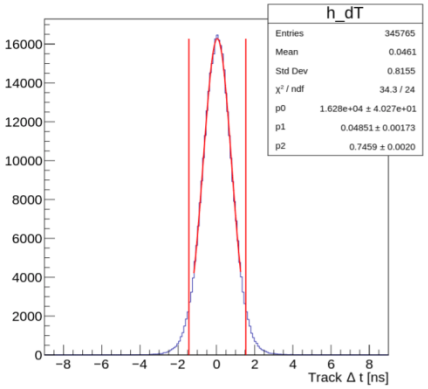

Data

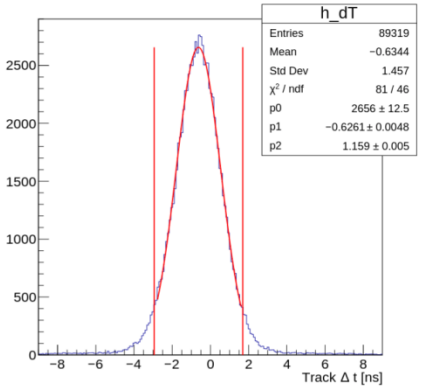

Momentum Sum

Monte Carlo

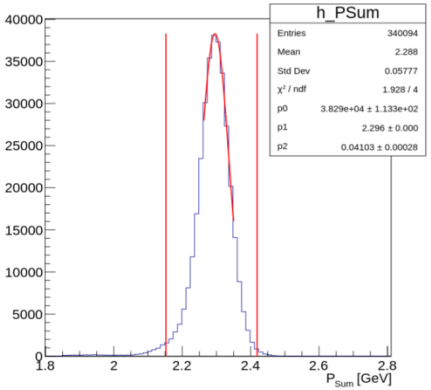

Data

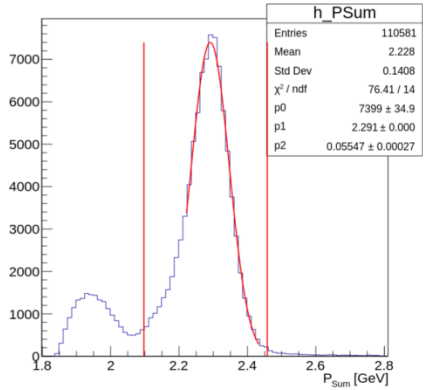

- Cut thresholds are set at 2σ of a Gaußian fit of the peak for each case.
  - An exception occurs for p_{sum} in data. In order to retain the radiative tail, the cut is instead set to 3.5σ on the lower end.
- Note: The bump is present in data and not Monte Carlo because the data contains all background processes while the Monte Carlo does not.

Møller Cluster/Track-Matching Cut

- A cluster/track-matching cut is also defined to reject tracks that match with a cluster by comparing the proximity of a cluster to the track position at the calorimeter face.
  - Like the previous cuts, a 2σ limit is used based on Gaußian fit of the distribution of these values.
  - Tracks pointing to the beam hole are required to have no associated cluster.

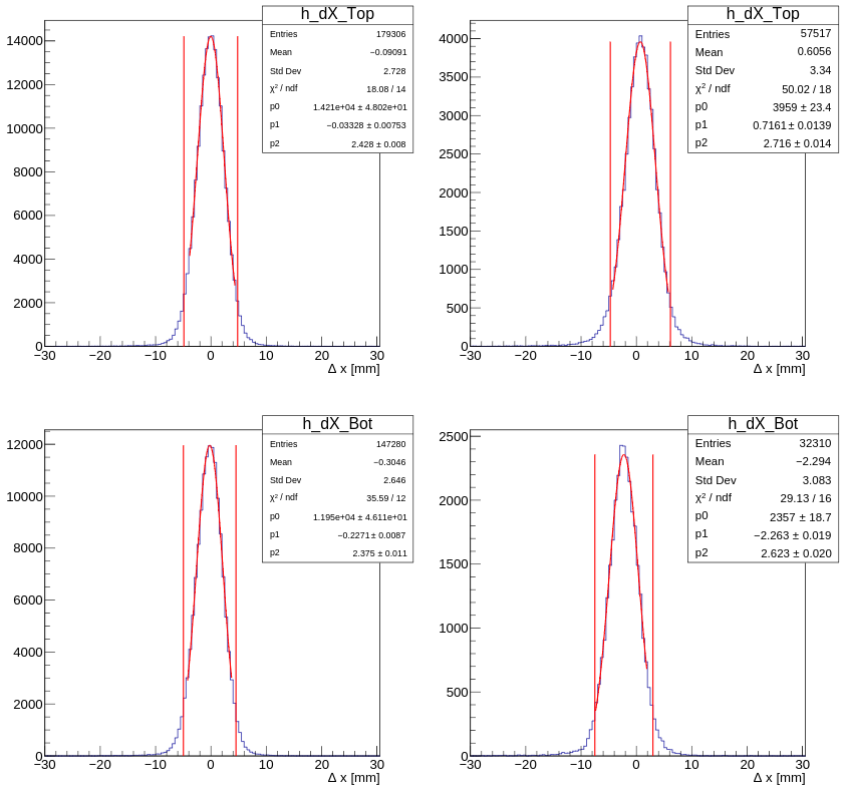

- This cut will eliminate many Møller events, but helps ensure a more pure sample.

Møller Mass Resolution

- The Møller mass resolution for data is roughly twice as wide as it is for Monte Carlo.

Monte Carlo

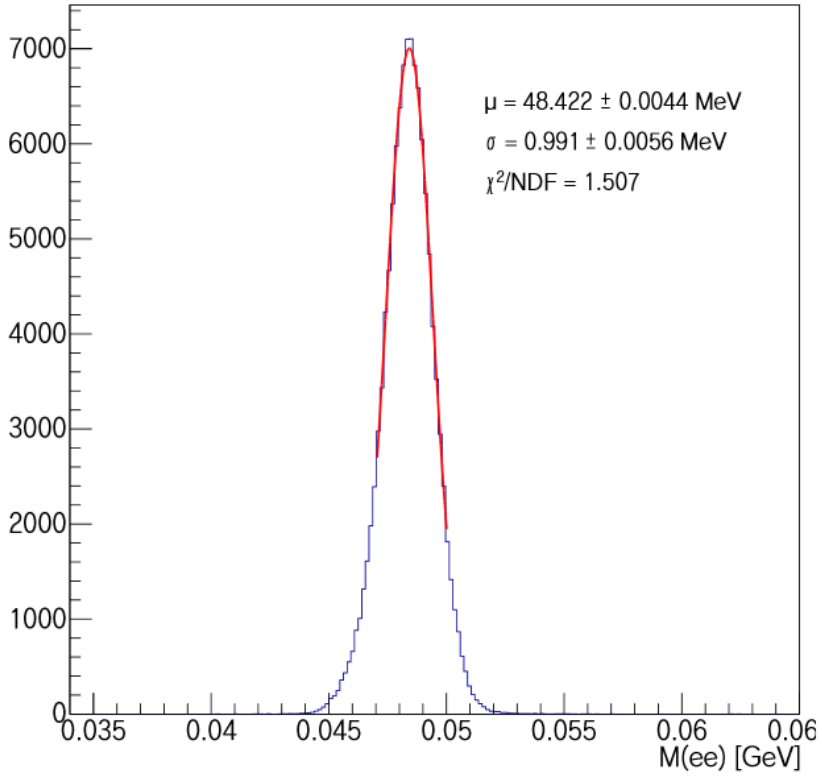

Data

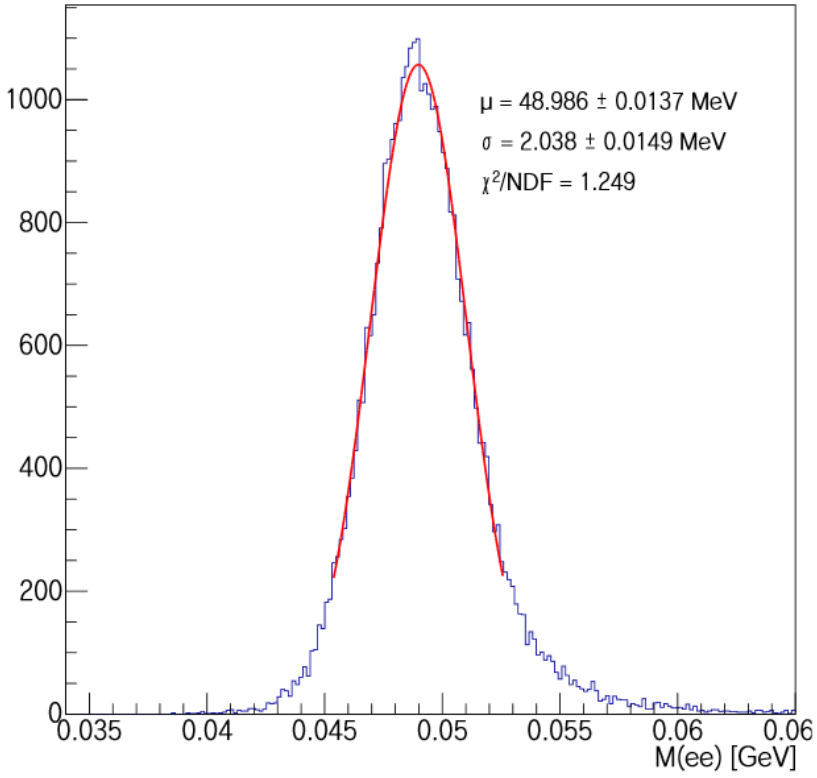

Sources of the Discrepancy

- It is important to understand and account for this discrepancy.
- The Møller mass may be defined as follows:

$$M(\mathrm{e^-e^-}) = 2\sqrt{p_1 p_2} \cdot \sin\left(\frac{\theta}{2}\right)$$

- There are two potential sources of the discrepancy:
  - Momentum resolution difference.
  - Angular resolution difference.

- It is assumed that the angular resolution is consistent between Monte Carlo and data.

- Full-energy electrons are useful for studying a momentum resolution difference.

Selection of Full-Energy Electrons

- For data, only events in which one of the singles triggers triggered are used. For Monte Carlo, the Møller beam sample is used, since it already contains full-energy electrons.
- A fiducial cut is then applied to the track *x*-coordinate of each sample.

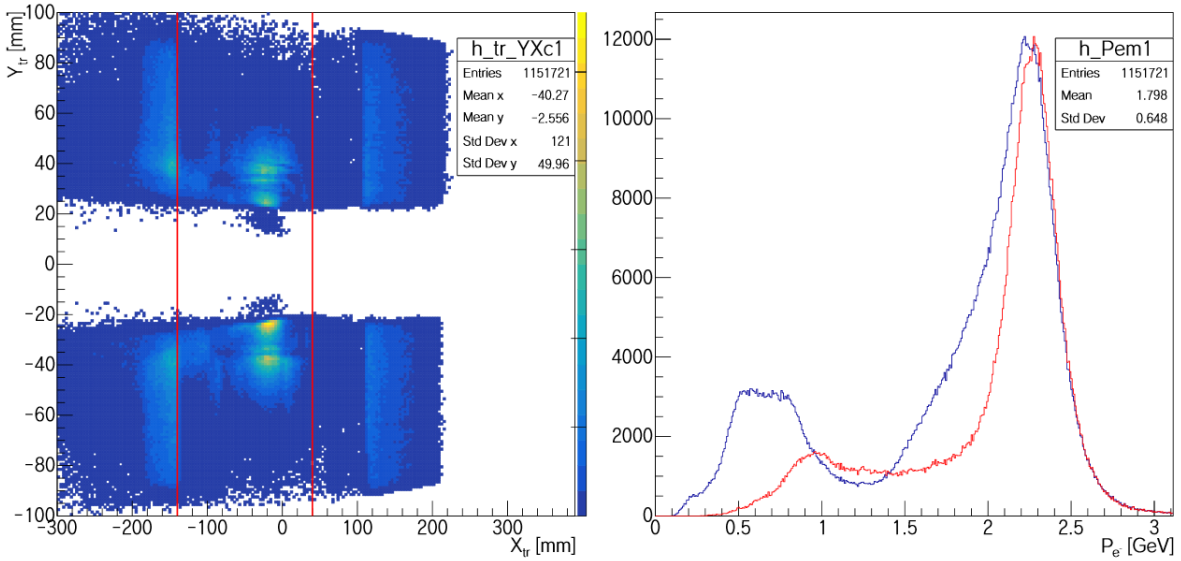

- On the right, the distribution before and after the cut is displayed for data. Note that the distribution is scaled to better show the improved peak.

Momentum Resolutions

- The momentum resolution varies depending on the whether a track has five or six hits and whether it is a top or bottom track.

5-Hit Tracks | **6-Hit Tracks**

	Monte Carlo	*Data*	*Monte Carlo*	*Data*
Top	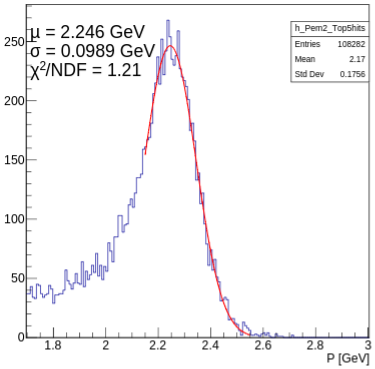	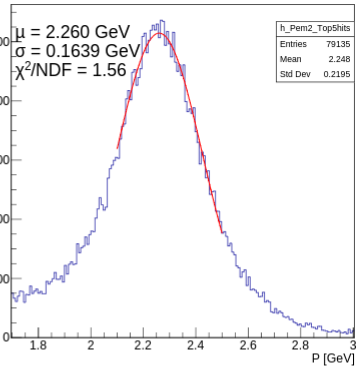	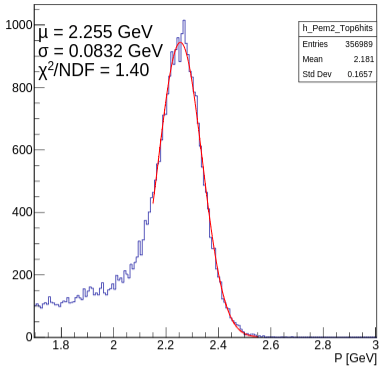	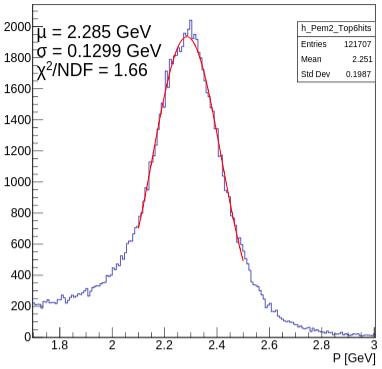
Bottom	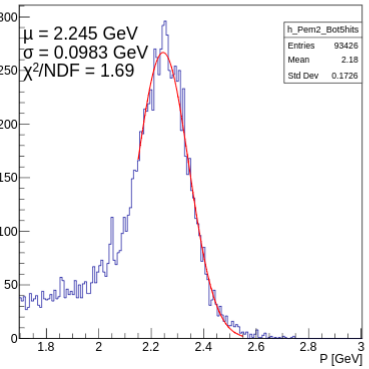	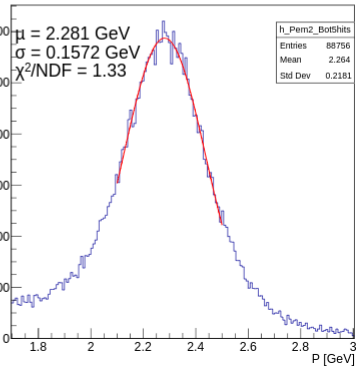	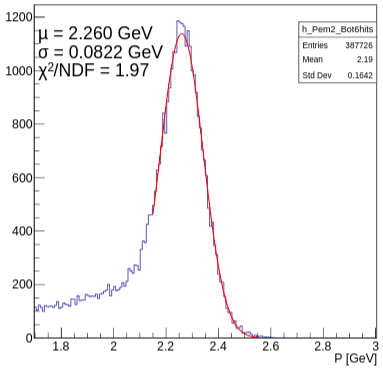	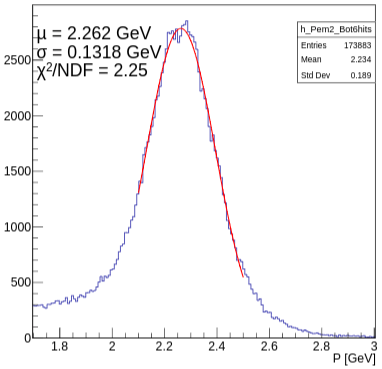

Momentum Resolution Correction

- 5-hit tracks have a 1.2 times wider resolution than 6-hit tracks, for both data and Monte Carlo.
- There are considerable differences between MC and data!
  - The full-energy electron momentum resolution in data is about 1.6 times wider than in Monte Carlo.
  - The mean values of the peaks are somewhat lower in Monte Carlo compared to data.
- Momentum smearing is used to correct this. The mass may be recalculated as follows:

$$M(\mathrm{e^-e^-}) = 2\sqrt{p_1^{\mathrm{smeared}} p_2^{\mathrm{smeared}}} \cdot \sin\left(\frac{\theta}{2}\right) = 2\sqrt{\frac{p_1^{\mathrm{smeared}}}{p_1^{\mathrm{rec}}} p_1^{\mathrm{rec}} \frac{p_2^{\mathrm{smeared}}}{p_2^{\mathrm{rec}}} p_2^{\mathrm{rec}}} \cdot \sin\left(\frac{\theta}{2}\right)$$

$$= \sqrt{\frac{p_1^{\mathrm{smeared}}}{p_1^{\mathrm{rec}}} \frac{p_2^{\mathrm{smeared}}}{p_2^{\mathrm{rec}}}} \cdot 2\sqrt{p_1^{\mathrm{rec}} p_2^{\mathrm{rec}}} \cdot \sin\left(\frac{\theta}{2}\right) = \boxed{M_{\mathrm{rec}}(\mathrm{e^-e^-}) \cdot \sqrt{\frac{p_1^{\mathrm{smeared}}}{p_1^{\mathrm{rec}}} \frac{p_2^{\mathrm{smeared}}}{p_2^{\mathrm{rec}}}}}$$

Smearing Comparison

- There is still not perfect agreement between data and Monte Carlo even after smearing.
  - Monte Carlo has a larger leading tail. This may be due to Møller in MC.
  - Data has larger trailing tails. This may be due to processes not well modeled in Monte Carlo.
- The core peaks do agree between the two, however.
- Note: Data and MC are scaled and centered to make comparison easier.

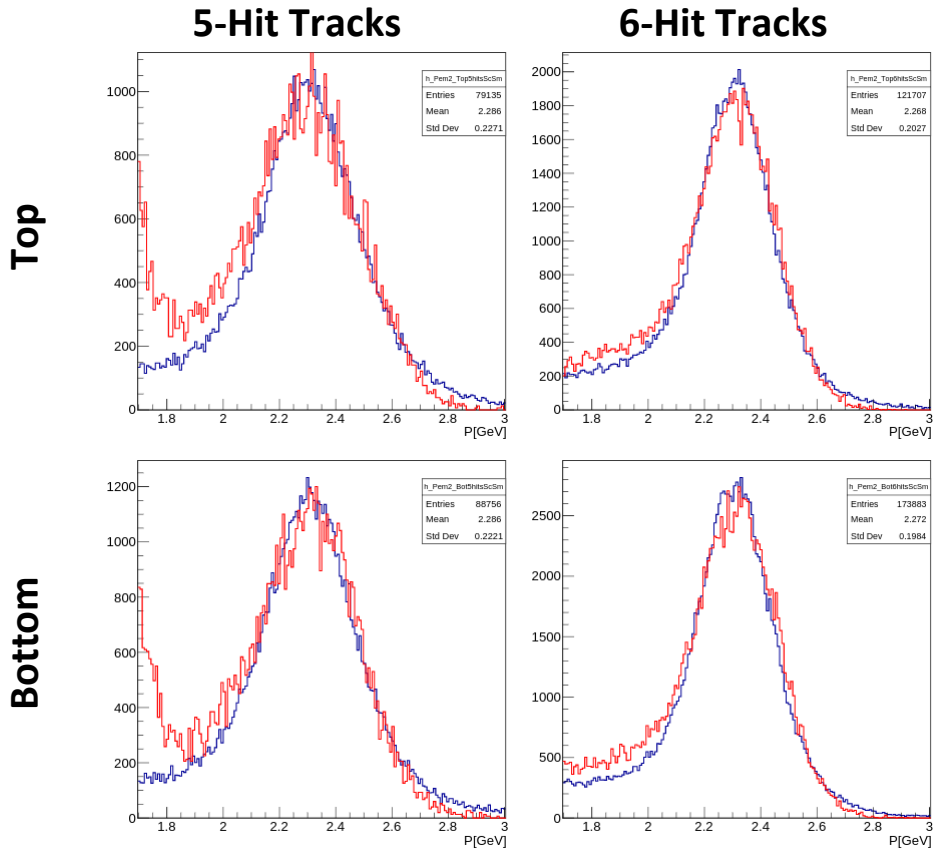

Smearing Comparison

- Smearing brings the Monte Carlo mass resolution significantly closer to the data mass resolution.

Monte Carlo (Unsmeared)

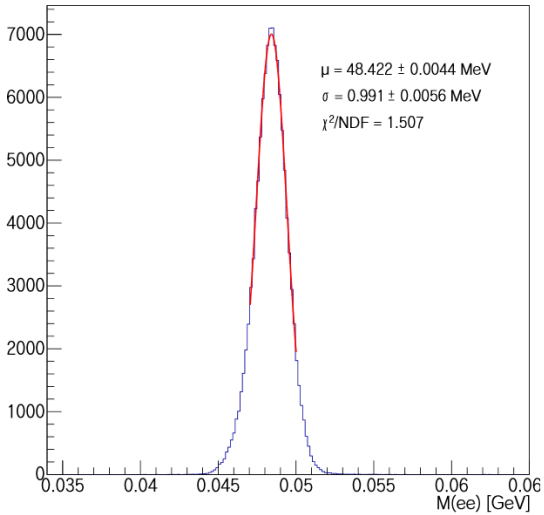

Data

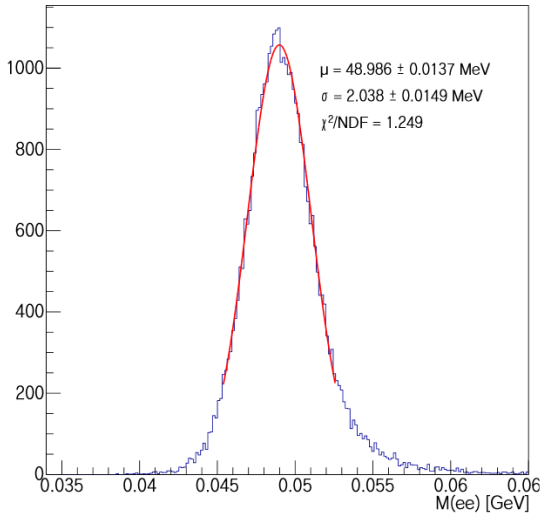

Monte Carlo (Smeared)

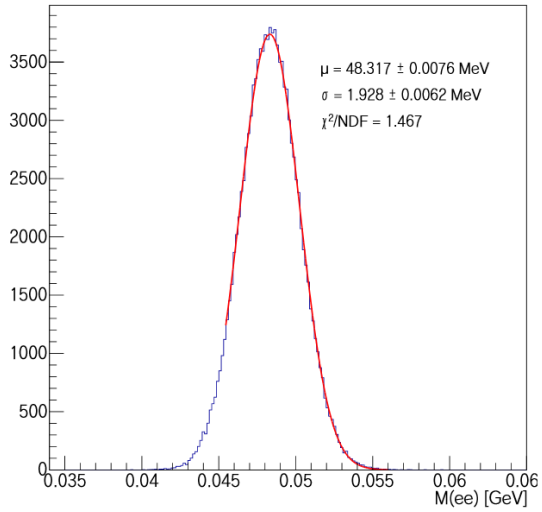

Final Mass Resolution

- The final mass resolution is defined as:

$$\sigma_m(m) = 0.000379509 + 0.0416842m - 0.271364m^2 + 3.49537m^3 - 11.1153m^4$$

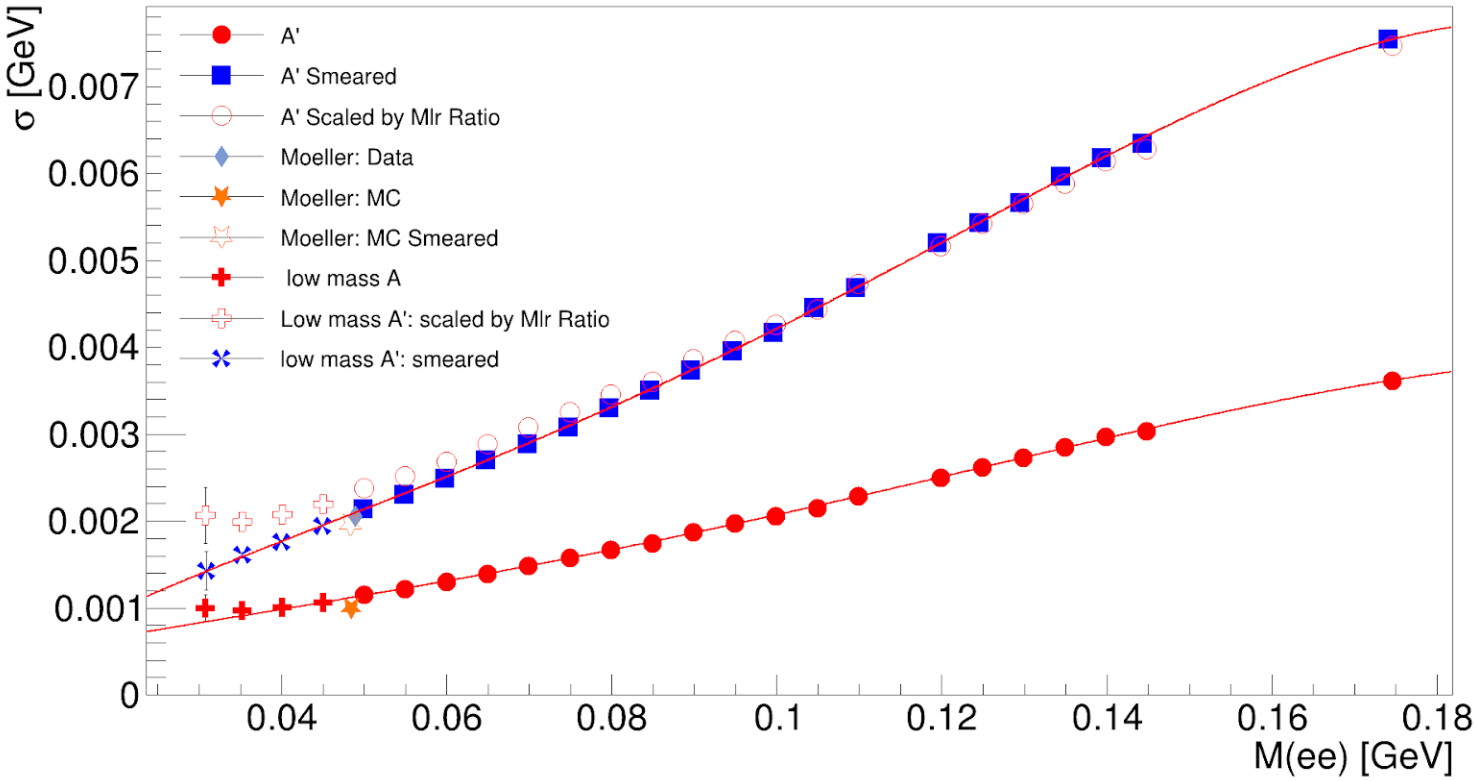

- Only the blue square points are used in the fit.

Part II: Radiative Fraction

Radiative Fraction

- The radiative fraction is derived from a combination of trident ("tritrig"), wide-angle Bremsstrahlung ("wab"), and radiative trident ("rad") MC.
  - The same selection cuts as applied to data are also applied to the MC.

- The electron particle with the most hits associated with its track is required to have a mother particle with PDGID 622 (the A') for radiative tridents.

- The reconstructed mass distribution of all samples is scaled to the 2016 luminosity.

- The ratio is taken of the above distribution and the A' reconstructed mass distribution taken from the radiative sample.

Radiative Fraction

- The resultant ratio is fit with polynomials from $\mathcal{O}(0) - \mathcal{O}(9)$ and an F-test is used to select the optimal fit.

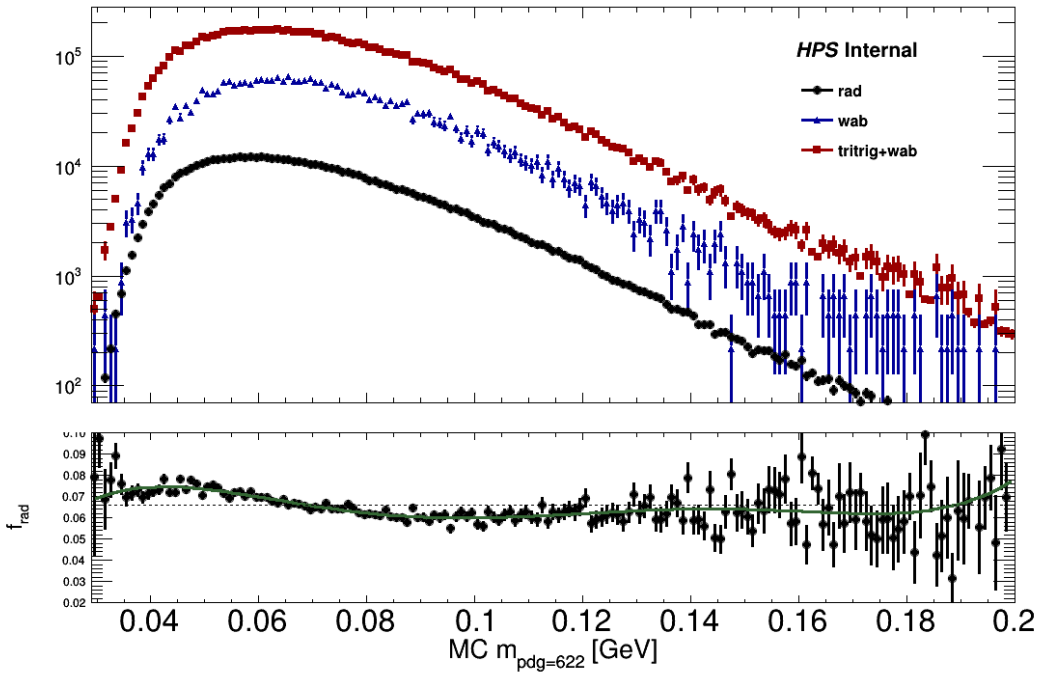

- An $\mathcal{O}(5)$ polynomial is found to fit best.

$$f_{\text{rad}}(m) = 13{,}603.8m^5 - 7{,}779.47m^4 + 1{,}669.07m^3 - 164.023m^2 + 7.0742m - 0.034465$$

Part III: Resonance Search and Results

Resonance Search Procedure

- A window $\left[m_{A'} - \frac{1}{2}[n_\sigma \times \sigma_m(m_{A'})], m_{A'} + \frac{1}{2}[n_\sigma \times \sigma_m(m_{A'})]\right]$ where n_σ is an integer scaling factor and $m_{A'}$ is the mass hypothesis, is selected.
  - n_σ is selected individually for each $m_{A'}$ as part of the background fit model selection process discussed later.
  - If the edge of the window would extend beyond the data, the window is instead shifted so that it begins at the end of the data, while remaining the same size.

- The window is then scaled such that it ranges from [-1, 1].
  - This is necessary to ensure the orthogonality of the background model fit polynomials.

Resonance Search Procedure

- A binned maximum likelihood fit is performed with two fit models.
  - The background-only fit model $10^{L_n(m)}$, where $L_n(m)$ are the Legendre polynomials of the first kind of order n.
    - n is selected during the background fit model selection process.
  - The signal + background fit, consists of the background-only fit model and a Gaußian with $\mu = m_{A'}$ and $\sigma = \sigma_m(m_{A'})$.

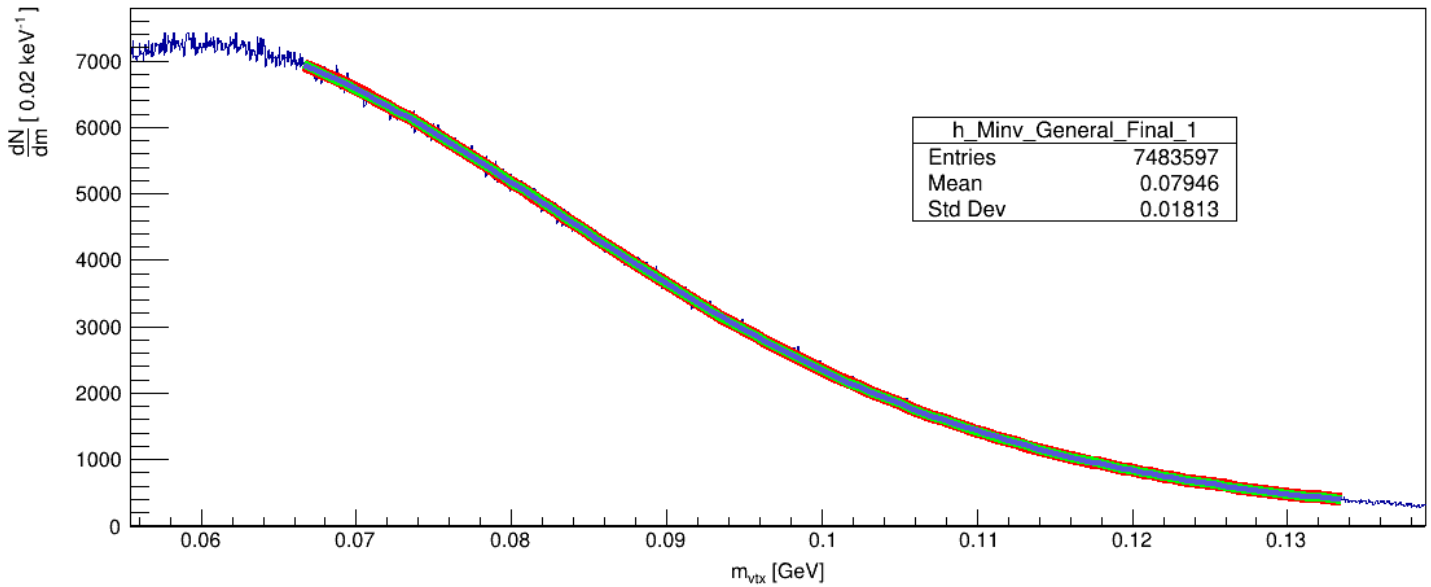

$m_{A'}$ = 100 MeV

n = 5

Resonance Search Procedure

- The p-value is calculated as it was in 2015.
  - If the signal yield $\hat{\mu}$ is negative, *p* is by definition 1.

- The upper limit calculation is defined by Cowen *et alii* as:

$$N_{\text{sig}}^{\text{up}} = \max(\hat{\mu}, 0) + \hat{\mu}_{\text{err}}\Phi^{-1}(1-\alpha)$$

  where $\Phi^{-1}(1-\alpha) = 1.64$ for a significance threshold of $\alpha = 0.05$.

- Lastly, ε^2 is calculated, where
  - $f_{rad}(m_{A'})$ is the radiative fraction.
  - $\left.\frac{dN_{\text{bkg}}}{dm}\right|_{m=m_{A'}}$ is the differential background rate.

$$\varepsilon^2 = \frac{2N_{\text{sig}}^{\text{up}}\alpha_{\text{EM}}}{3\pi m_{A'} f_{\text{rad}}(m_{A'}) \left.\frac{dN_{\text{bkg}}}{dm}\right|_{m=m_{A'}}}$$

Background Model Selection – Study

- Models are selected via the results of a study of 10% of the data.
- Toy models are produced with the following parameters:
  - Mass hypothesis $m_{A'}$ = [39, 180) MeV in 1 MeV steps.
  - $\mathcal{O}(3)$ and $\mathcal{O}(5)$ background fit polynomials of the form $10^{L_n(m)}$.
  - Window sizes from $5\sigma_m$ – $30\sigma_m$.
  - 10,000 toys are thrown using a fit of the form $10^{L_{n+2}(m)}$, with the same statistics as the 10% data set.
  - No signal is injected.
- Signal yield, signal yield error, and pulls are plotted from fits to the toys.
- The p-value, background-only fit χ^2, signal + background χ^2, and toy generator fit χ^2 are plotted from the fits to 10% of the data.
- Limits for ε^2 are calculated and plotted.

Background Model Selection – Selection Plots

- Example results for 100 MeV for $\mathcal{O}(3)$ and $\mathcal{O}(5)$.

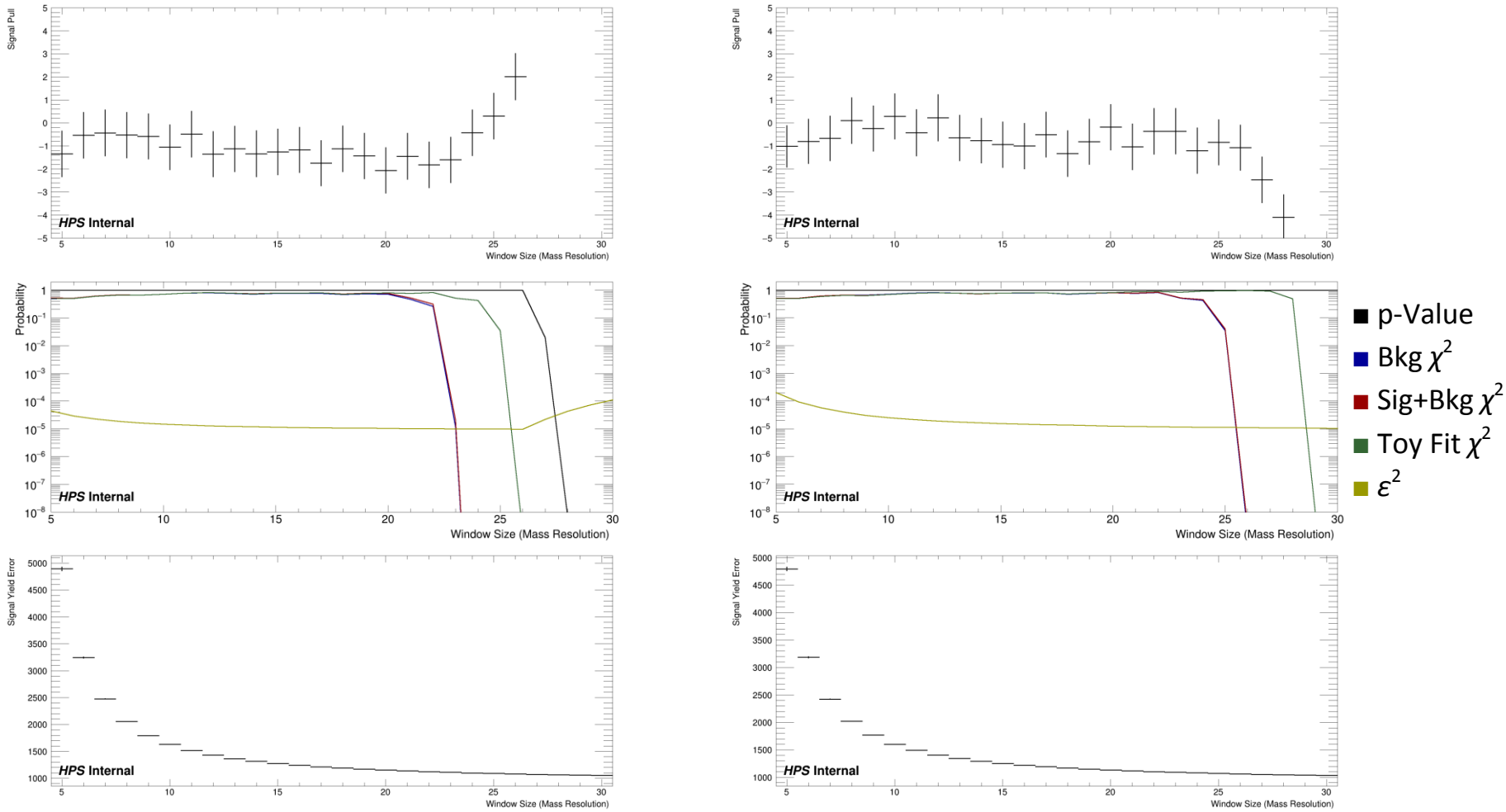

Background Model Selection – Methodology

- A background model was selected by considering the summary plots of each mass hypothesis. A good model meets the following conditions:
  - χ^2_{bkg} probability > 0.01 – The background-only fit should be fairly accurate.
  - Pull within $2\sigma_{\text{RMS}}$ of zero – It is expected that no signal will be visible at 10% statistics.
  - Stability – The selected model should be centered in the set of potentially usable windows to avoid instability.
  - All other things equal, a lower order is preferred.

Background Model Selection – Stability

- Lastly, stability and model order are considered.

- A model is considered stable if it is in the center of a range of consecutive models which all have acceptable values for both pull and χ^2_{bkg}.
  - Stability is better the larger this range is, as it places the selected model farther from the edges of the stable region.
  - Some threshold is needed to determine what qualifies as a "sufficiently large stable region." A threshold if 5 is selected for this study.

- In the event that there are multiple orders that have acceptable ranges, the lower order is preferred as it is less likely to over fit.

- If no order has a large enough range, the center of the largest range is selected.

Background Model Selection – Compiled Results

Mass	Order	Window	Mass	Order	Window	Mass	Order	Window	Mass	Order	Window	Mass	Order	Window
39	5	18	68	3	7	97	3	13	126	3	13	155	3	8
40	5	19	69	5	11	98	3	13	127	3	13	156	3	7
41	5	14	70	5	11	99	3	13	128	3	13	157	3	9
42	5	13	71	5	11	100	3	12	129	3	12	158	3	7
43	5	13	72	5	11	101	3	10	130	3	12	159	3	8
44	5	11	73	5	11	102	3	11	131	3	12	160	3	8
45	5	12	74	3	8	103	3	11	132	3	12	161	3	8
46	5	12	75	3	8	104	5	14	133	3	12	162	3	9
47	5	8	76	3	8	105	3	10	134	3	12	163	3	8
48	5	8	77	3	9	106	3	10	135	3	12	164	3	9
49	5	9	78	3	9	107	3	10	136	3	12	165	3	8
50	5	9	79	3	9	108	3	11	137	3	12	166	3	8
51	5	8	80	3	10	109	3	10	138	3	12	167	3	9
52	5	8	81	3	10	110	3	11	139	3	12	168	3	10
53	5	8	82	3	10	111	3	11	140	3	12	169	3	9
54	5	9	83	3	11	112	3	11	141	3	9	170	5	10
55	5	9	84	3	11	113	3	14	142	3	10	171	3	9
56	5	9	85	3	12	114	3	14	143	3	9	172	5	10
57	5	9	86	3	7	115	3	14	144	3	9	173	3	10
58	5	9	87	3	12	116	3	14	145	3	9	174	3	9
59	5	9	88	3	12	117	3	14	146	3	8	175	5	10
60	5	10	89	3	12	118	3	14	147	3	8	176	3	9
61	5	9	90	3	12	119	3	14	148	3	9	177	5	9
62	5	9	91	3	12	120	3	14	149	5	13	178	3	9
63	3	8	92	3	14	121	3	14	150	3	8	179	3	11
64	3	8	93	3	13	122	3	14	151	3	8			
65	3	8	94	3	14	123	3	14	152	3	8			
66	3	7	95	3	13	124	3	13	153	3	8			
67	3	7	96	3	13	125	3	13	154	3	8			

Preliminary Limits

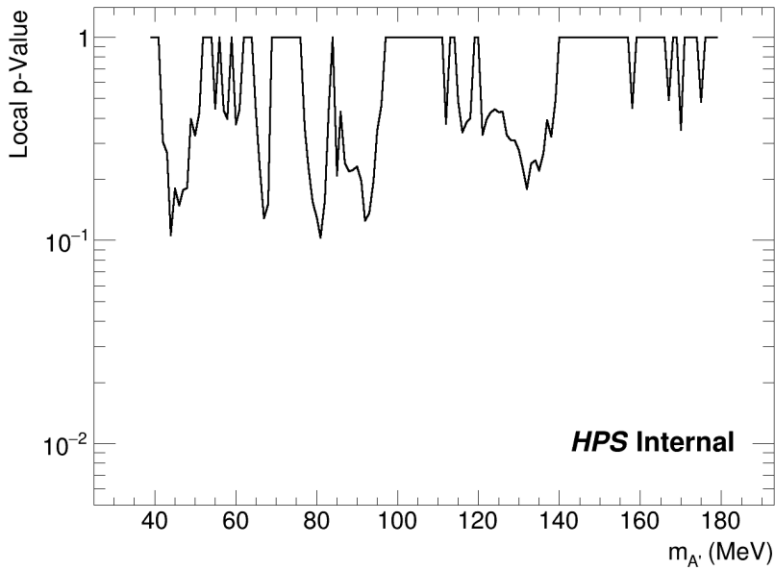

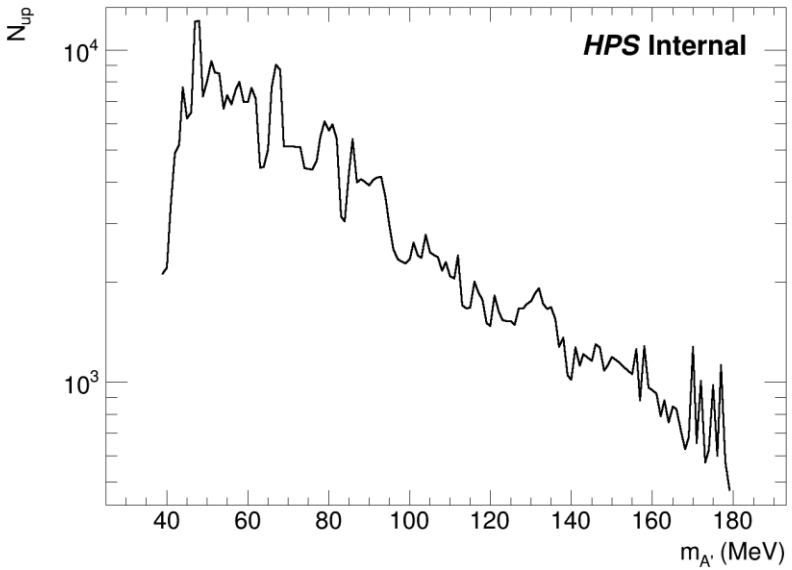

- By Gross and Vitells in "Trial factors for the look elsewhere effect in high energy physics," the global p-value can be approximated by scaling by the average of the mass resolution within the full search window (39 MeV – 180 MeV) divided by the width of the full search window.

- The global p-value is approximately 30 times larger (divide by 0.034).
  - This translates to a global p-value is effectively 1.00.

Preliminary Limits

- The ε^2 limit is plotted in a different manner with toy limit quantiles.

- A series of 10,000 toys are generated for the selected for models, using a toy generator fit function of $10^{L_n(m)}$.
  - The ε^2 limit is calculated for each of the toy distributions.
  - The median ε^2 limit is plotted.
  - The 68% and 95% quantiles are also plotted.

- This procedure is then repeated with the same parameters, but 10x statistics to produce an expected range for an unblended analysis.

Preliminary Limits

- The ε^2 limit is plotted with data and toy distribution results for 1x statistics.

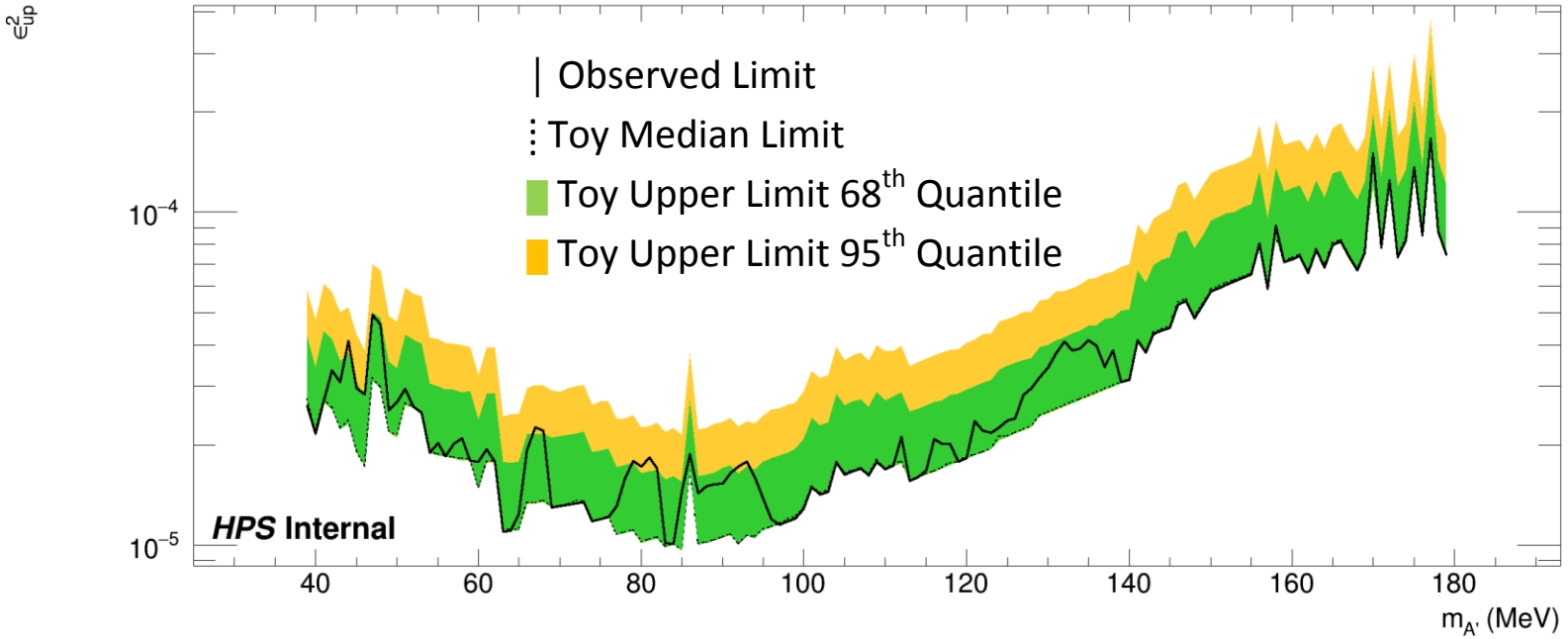

- The observed ε^2 limit is within the expected range.
- Many toy distributions produced a negative pull, which results in the lower range 95th quantile often being equivalent in value to the 68th quantile results.

Preliminary Limits

- The ε^2 median limit and quantiles are shown for fits on 10x statistics toys.

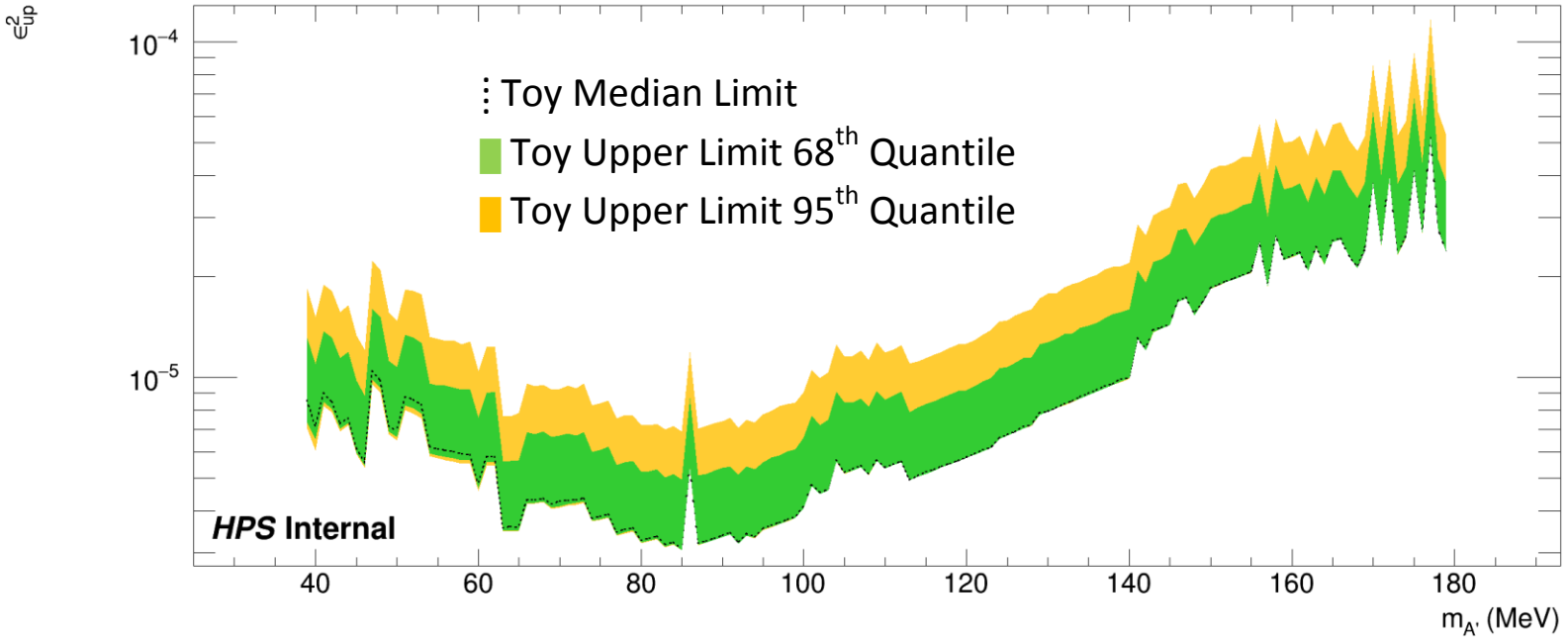

- Again, many toy distributions produced a negative pull, which results in the lower range 95th quantile often being equivalent in value to the 68th quantile results.

Part IV: Systematics

Systematic Uncertainty in the Mass Resolution

- Two main sources of uncertainty were identified with regards to the mass resolution. These are:
  - Uncertainty in the target position.
  - Uncertainty in the momentum smearing.

- Monte Carlo assumes a target position at nominal position, so any shift will result in differences between the Monte Carlo and data.

- Momentum smearing is used to bring Monte Carlo into alignment with data, and so likewise may induce uncertainty.

Target Position Systematics

- The mass resolution is calculated with the target at ± 0.5 mm.

Mass Resolution

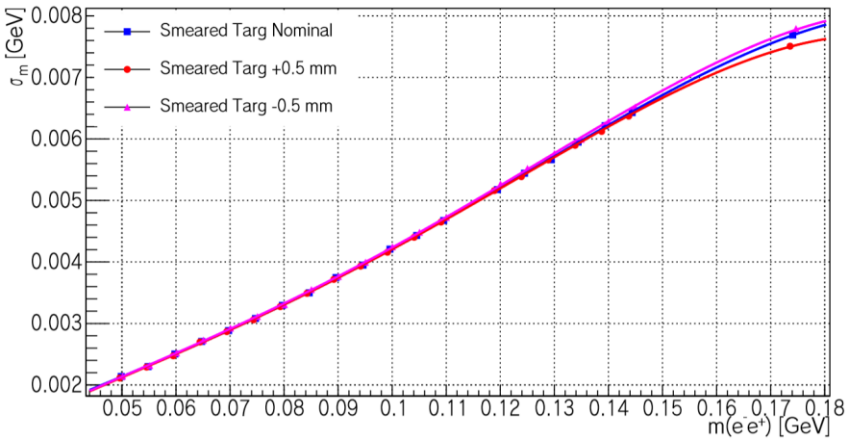

Systematic Errors

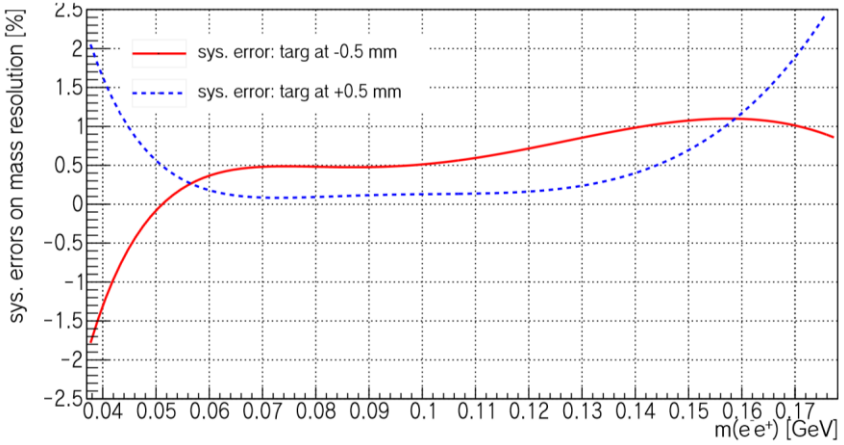

- The systematic is the maximum value of the curves.
- This 2.5%, which occurs at 179 MeV for +0.5 mm.

FEE σ Cut Systematics

- The mass resolution is calculated with smearing values set to ± 1σ.

Mass Resolution

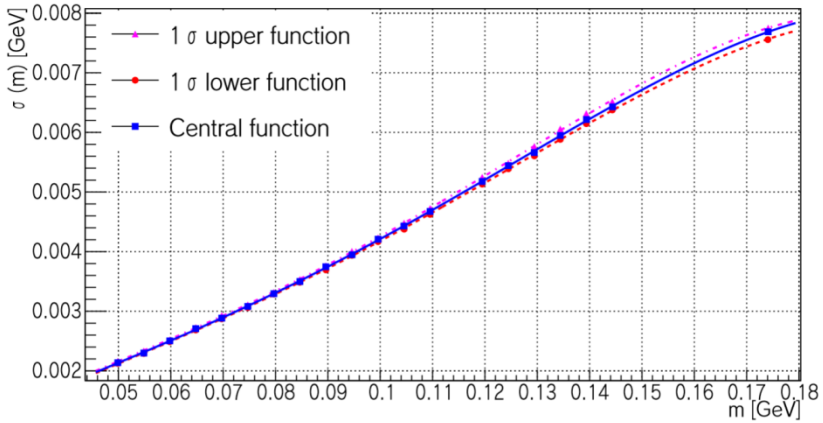

Systematic Errors

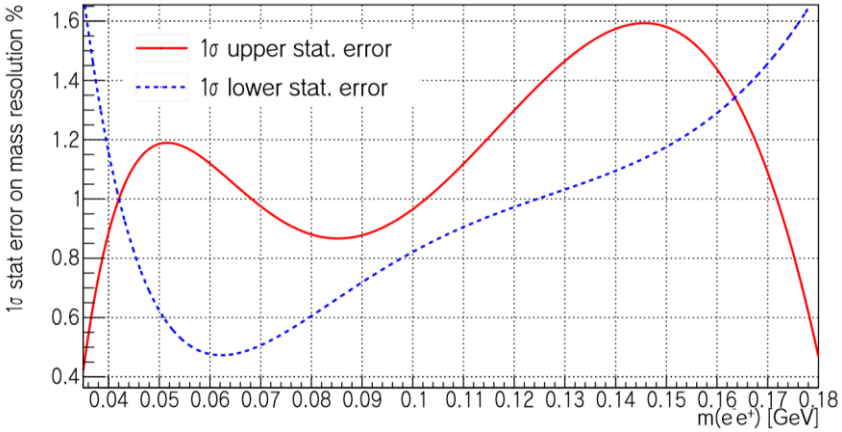

- Again, the systematic is the maximum value of the curves.
- The maximum difference is 1.6%, occurring at 179 MeV.

Systematic Uncertainty in the Mass Resolution

- Because the uncertainties that contribute to the mass resolution are independent, the total uncertainty can be defined as the sum in quadrature of the two individual errors.

$$\mathrm{Err}_{\mathrm{total}} = \sqrt{\mathrm{Err}^2_{\mathrm{target}} + \mathrm{Err}^2_{\mathrm{smear}}}$$

- This is found to be 3.4%.

Systematic Uncertainty in the Mass Resolution

- The effect of a variation in the mass resolution is explored to get an idea of how significant uncertainty is.

- Consider a study where:
  - Mass hypothesis $m_{A'}$ = { 55, 100, 175 }.
  - The background model selected for each mass is used.
  - 1,000 toys are thrown.
  - 10^4 signal events are injected.
  - Mass resolutions of [$0.90\sigma_r$, $1.10\sigma_r$] in intervals of $0.05\sigma_r$ are used.

- The pull is calculated and plotted for each mass resolution.

Systematic Uncertainty in the Mass Resolution

$m_{A'} = 55$
$\mathcal{O}(5)$
$n_\sigma = 9$

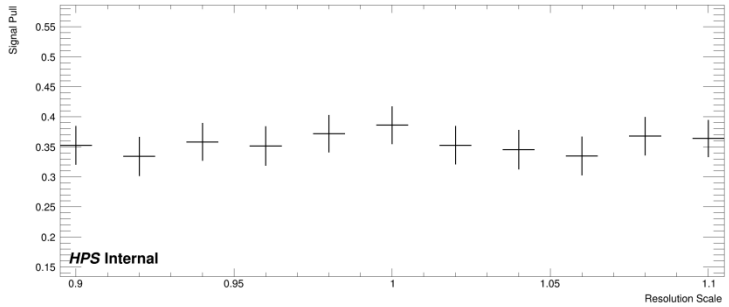

$m_{A'} = 100$
$\mathcal{O}(3)$
$n_\sigma = 12$

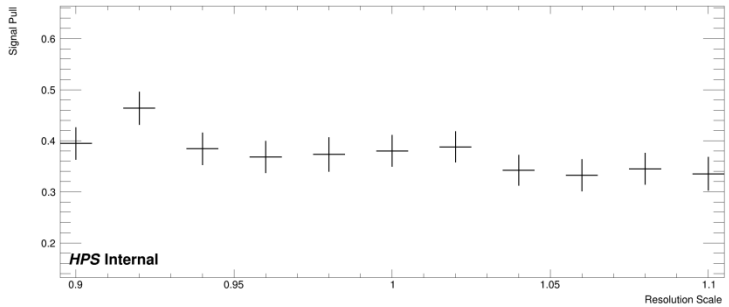

$m_{A'} = 175$
$\mathcal{O}(5)$
$n_\sigma = 10$

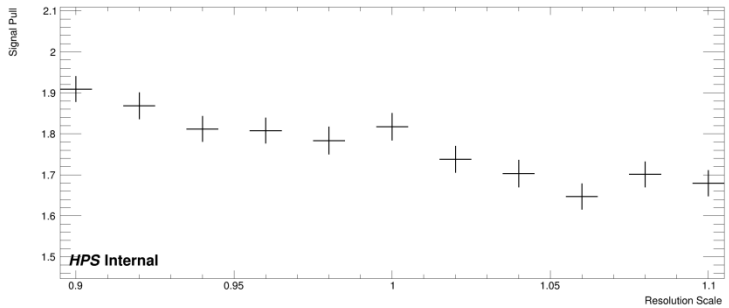

- The pull is quite stable, indicating that inaccuracies in the mass resolution of up to 10% will have little effect; at most, 1% per percent change.

Other Systematics and Effects

- Uncertainty in WAB Monte Carlo distributions is expected to produce a roughly 6% systematic.

- The systematics for the radiative fraction are currently being studied.

- Modification of the analysis to account for systematics in the calculation of the final limits will be performed once systematics are completed.

[END]

Appendix A: Data Selection

Run Conditions

- Data is taken from the HPS 2016 run from February to the end of April.
  - Data taking occurred only on weekends.
  - HPS used a 200 nA at 2.3 GeV and a 4 μm Tungsten target.

- Data was selected from "golden runs."
  - Production trigger
  - 200 nA current
  - No major livetime issues present
  - SVT at nominal position

- Every 10 files (ending in -0, *id est* 10, 20, 30) were used for a blind analysis.

Run Summary

Runs	Total Luminosity (nb^{-1})	Blind Luminosity (nb^{-1})	Total Files	Blind Files
81	10,703.810	1,096.2709	15,934	1,625

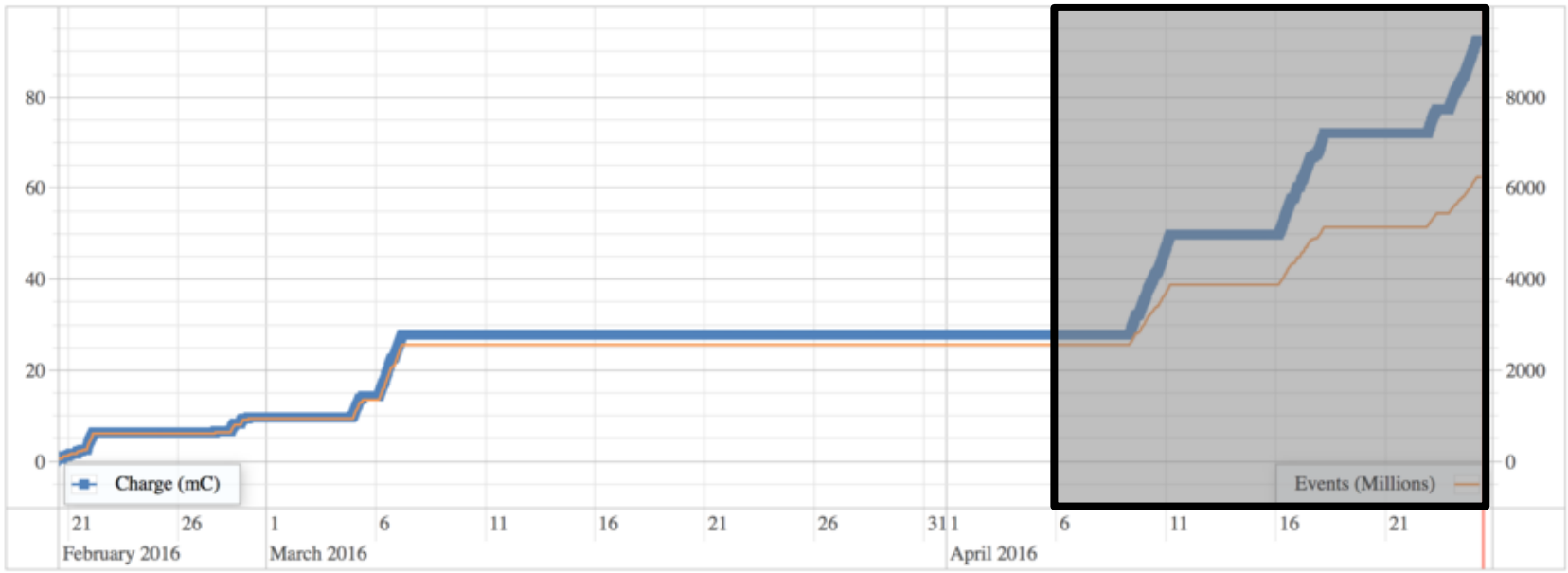

- Most data originates from the shaded region.

Electronic Calorimeter

- The HPS calorimeter is composed of 442 crystals, 221 on the top and bottom, with a central gap to allow the beam to pass and a 9 crystal “beam hole” where occupancies were too high.
- Dipole magnets are used such that the electron from an A’ decay travels to one half of the calorimeter and the positron to the other. Kinematically, one of the particles travels to the top and one to the bottom.

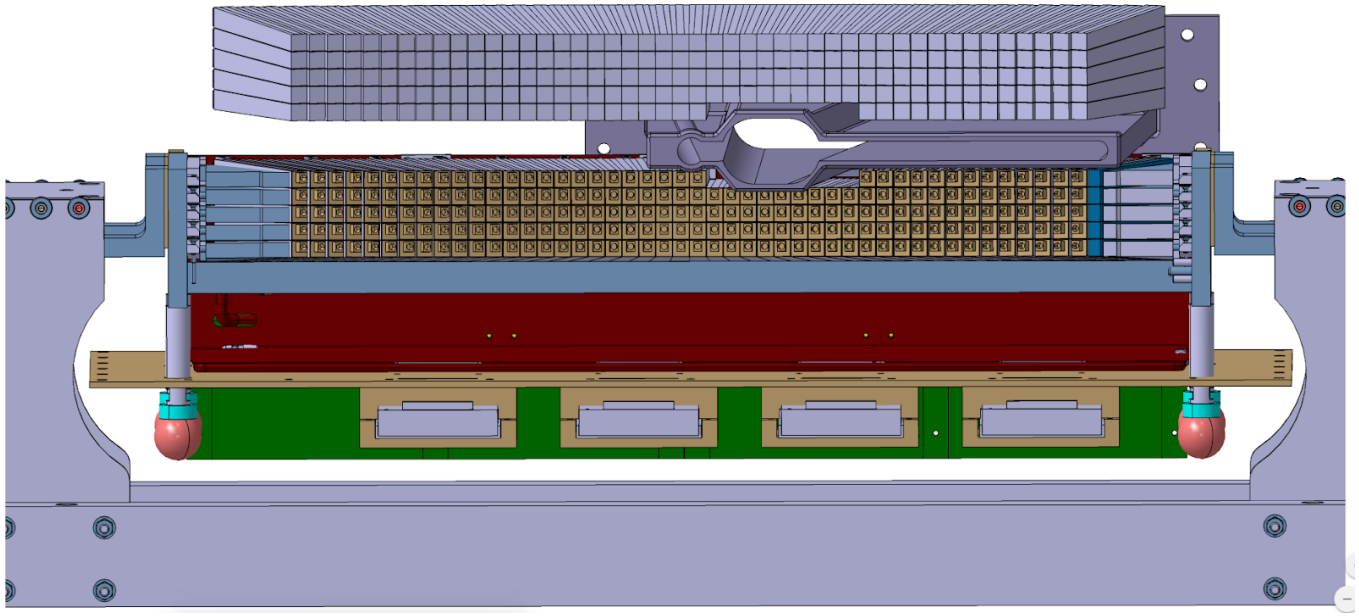

Production Trigger

- The HPS production trigger operated with the following settings:
  - $0.150\ \text{GeV} \leq E_{\text{cluster}} \leq 1.400\ \text{GeV}$
  - $N_{\text{hits}} \geq 2$
  - $0.600\ \text{GeV} \leq E_1 + E_2 \leq 2.000\ \text{GeV}$
  - $|E_1 - E_2| \leq 1.140\ \text{GeV}$
  - $E_{\text{low}} + (0.0055\ {}^{\text{GeV}}/_{\text{mm}}) \cdot r_{\text{low}} \geq 0.700\ \text{GeV}$
  - $|\tan^{-1}(x_1 / y_1) - \tan^{-1}(x_2 / y_2)| \leq 35°$
  - $|t_1 - t_2| \leq 12\ \text{ns}$

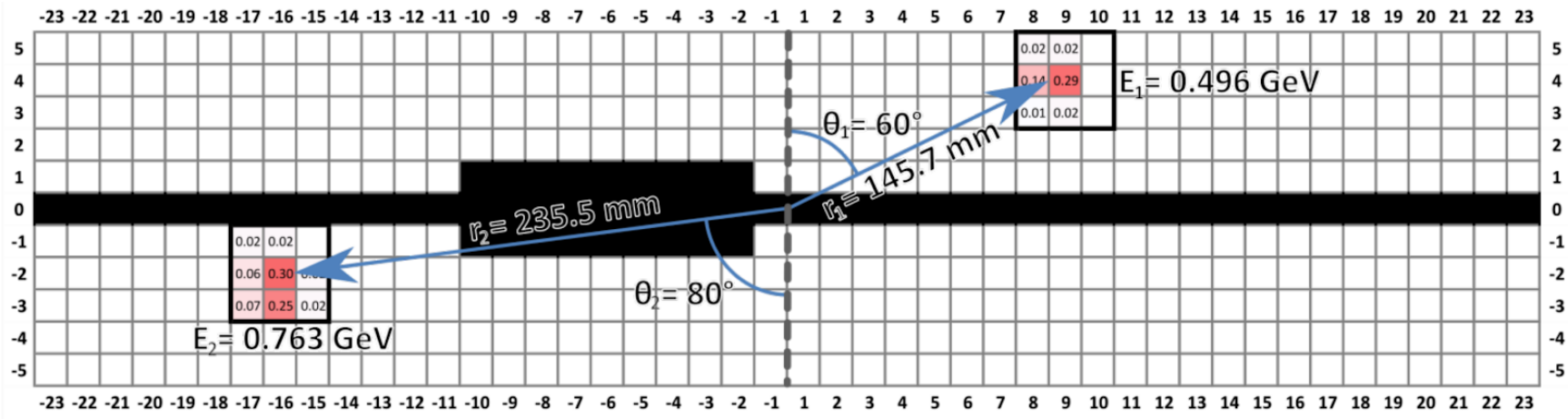

Preselection of Events

- Event selection begins with the loose, reconstruction-level "MOUSE" cuts, which select "V_0 candidate" vertices. These consist of two particles where:
  - One points to the top and one the bottom of the calorimeter.
  - One is positively charged and one is negatively charged.
- There are several cuts which depend on the particle type.

Electron	Positron
• Negative track • $\chi^2 < 12$ • Goodness of PID < 10 • $\lvert\Delta t_{track}\rvert < 6$ ns • $p < 2.15$ GeV	• Positive track • $\chi^2 < 12$ • Goodness of PID < 10 • $\lvert\Delta t_{track}\rvert < 6$ ns

- Additionally, all tracks use the target position as a constraint in track formation.

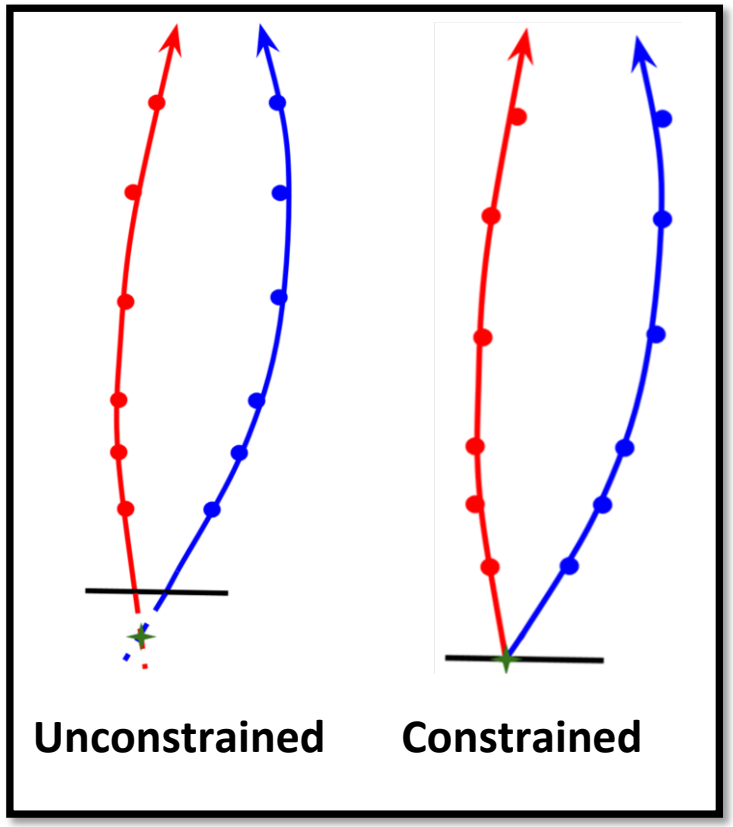

Cluster Timing Cut

- Timing cuts are applied to select the cluster which caused the trigger.
  - Trigger time is set by the bottom cluster.
  - Data has an energy-dependent cut due to time walk effects.
  - Time-walk is not properly emulated in MC, so it does not.

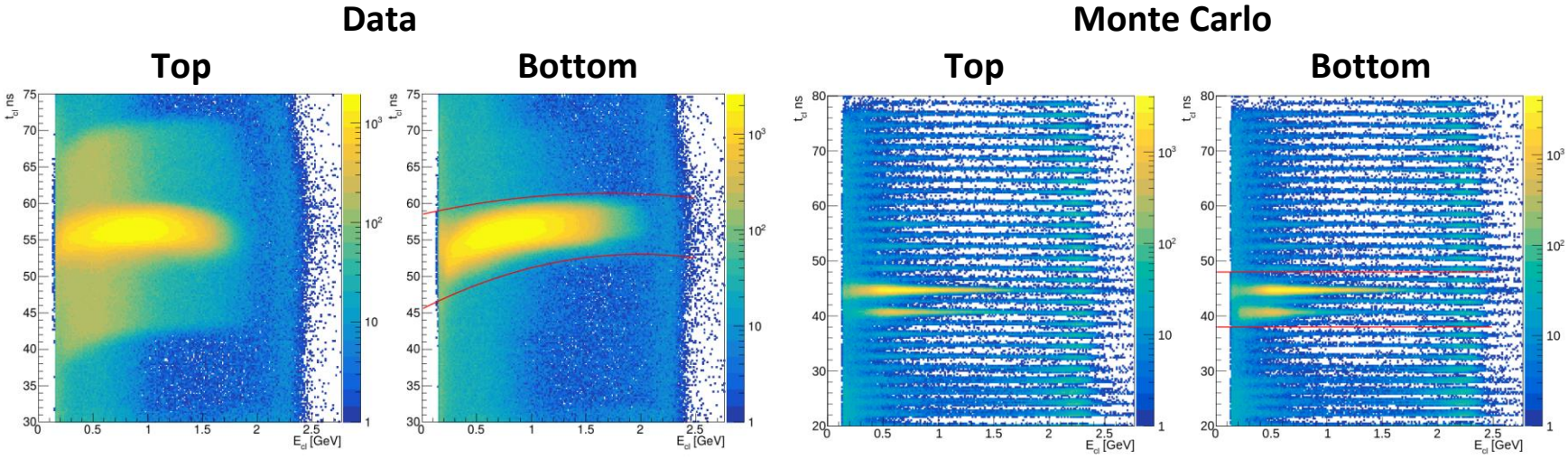

- The data cut is parameterized, with E in units of GeV, as $a + b \cdot E + c \cdot E^2$.
  - Upper Limit: a = 58.50, b = 3.40, c = -1.00
  - Lower Limit: a = 45.51, b = 7.55, c = -1.90

Aside: Time Corrections

- There are time offsets for some crystals. Consider a plot of the time difference between and the others.

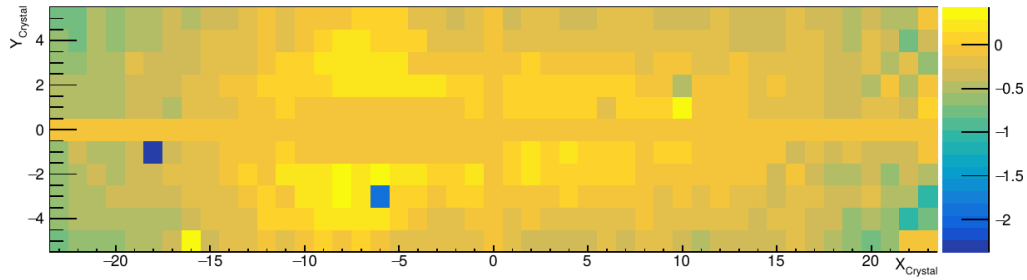

- There are different time offsets:
  - Two crystals have a 2 ns time difference.
  - Several have a few hundred picosecond offsets.

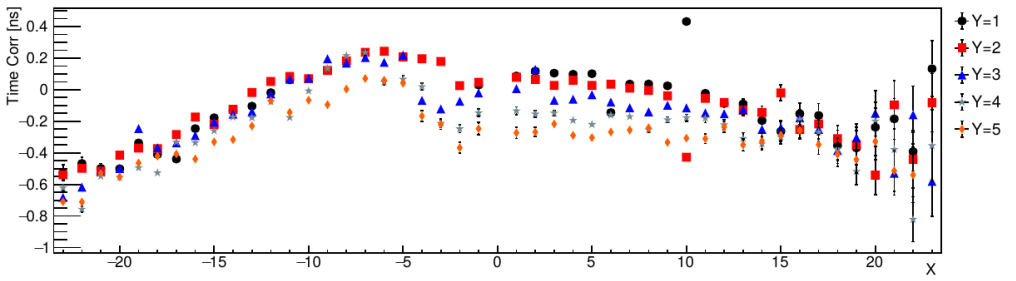

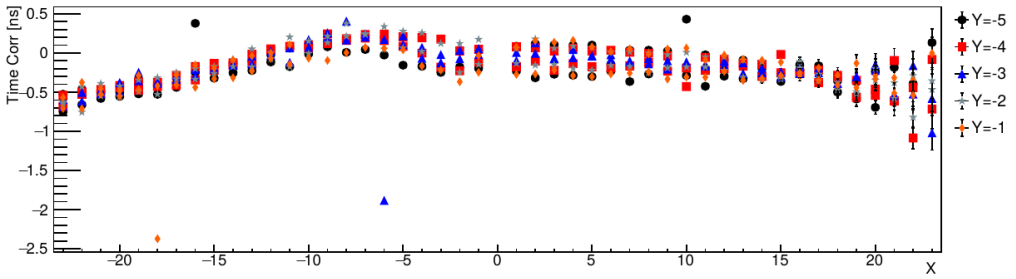

- There is an *x*-dependence, which is likely an energy-dependence.

Aside: Time Corrections

- The crystal times are corrected by the observed offsets.
  - The asymmetry in the tail disappears.
  - The peaks and valleys become more defined.
- Overall, the time resolution is improved by the corrections.
- The time corrections are only applied to data.

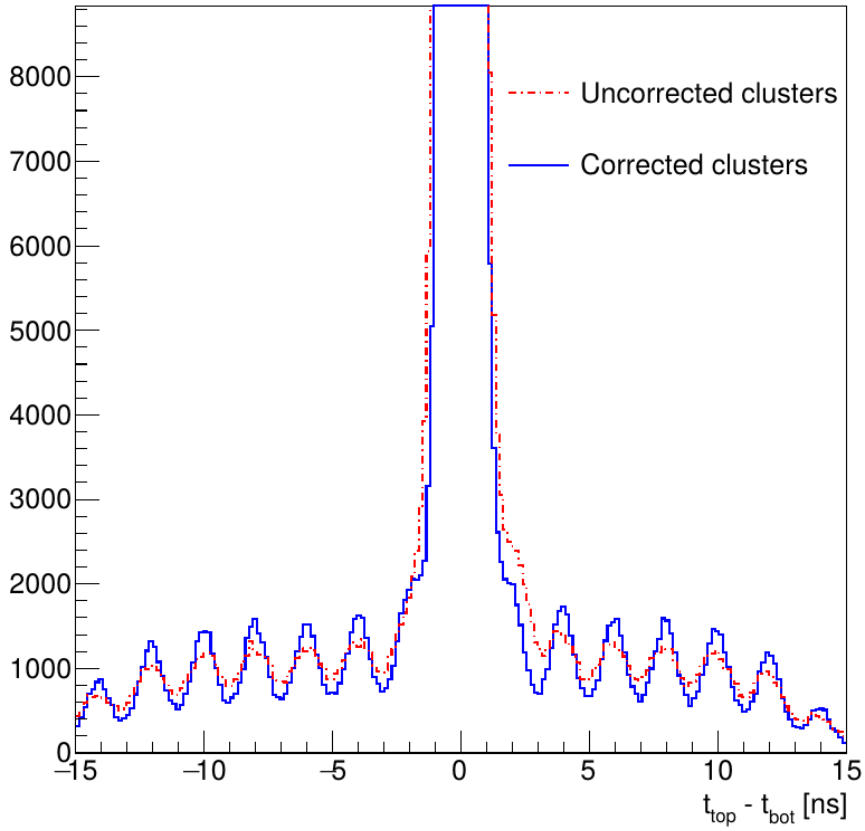

Time Difference Cut

- Each peak in the cluster time difference distribution is modeled as the sum of two Gaußian functions with the same mean values. The ratio of the peaks is the same for all peaks.

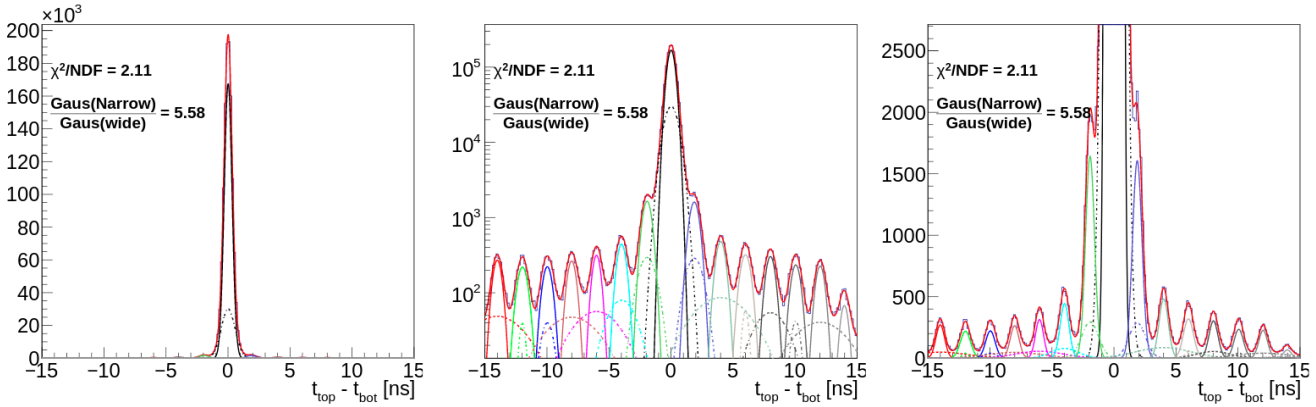

- The figure of merit is defined as $S_{\text{peak}}/\sqrt{S_{\text{total}}}$, where S_{peak} is the integral of the central peak, and S_{total} is the integral of all functions.
  - The cut is placed at $|\Delta t_{\text{track}}| < 1.43$ ns.

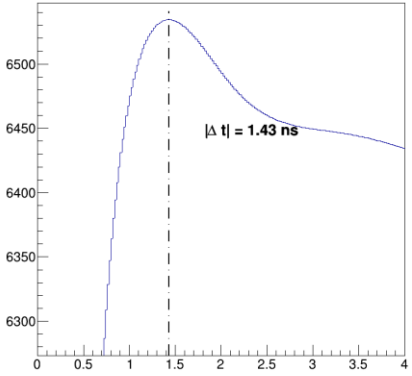

Momentum Sum Lower Bound Cut

- Differences in the momenta of processes can be used to clean the signal.
- A figure of merit can be defined as (with N being the integral of the relevant process of the below histogram):

$$\frac{N_{A'}}{\sqrt{N_{\text{total}}}} \equiv \frac{\mathcal{K} \cdot N_{\text{radiative}}}{\sqrt{N_{\text{total}}}} \propto \frac{N_{\text{radiative}}}{\sqrt{N_{\text{total}}}}$$

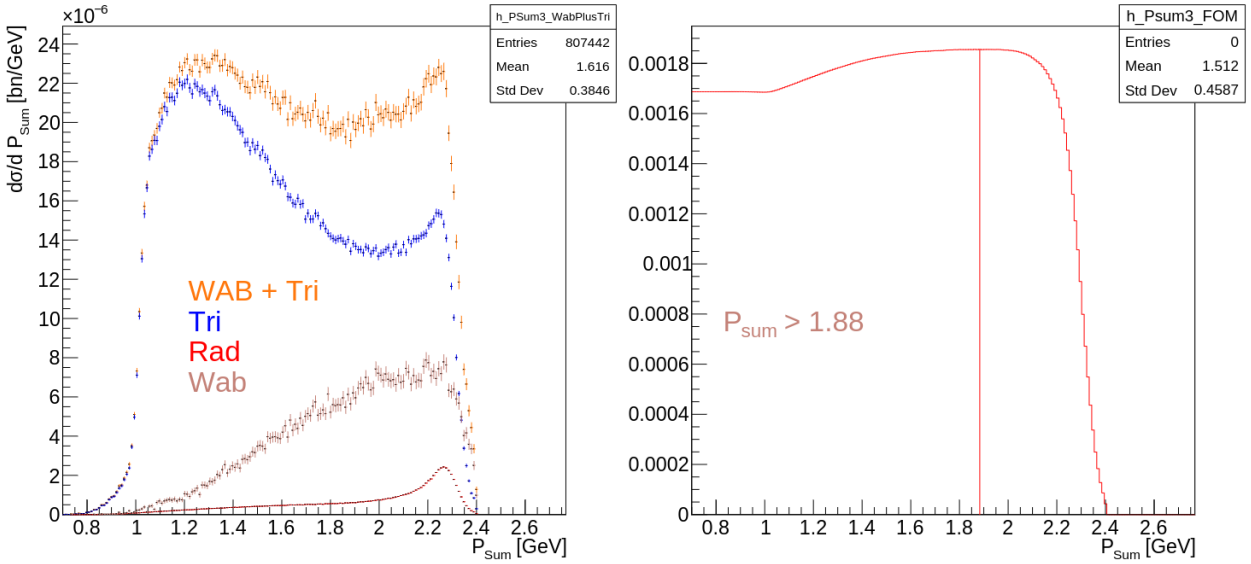

- The final cut is set to $p_{\text{sum}} > 1.9$ GeV for simplicity.

Additional Cuts

- Additional accidentals may be removed with an upper bound cut.
  - Radiative and trident samples have a sharp cut-off at 2.4 GeV, while wide-angle Bremsstrahlung has tails in this region.
  - Good alignment between the tails in data and MC suggests that this tail in data is also WAB.
  - A cut of $p_{sum} < 2.4$ GeV is applied.

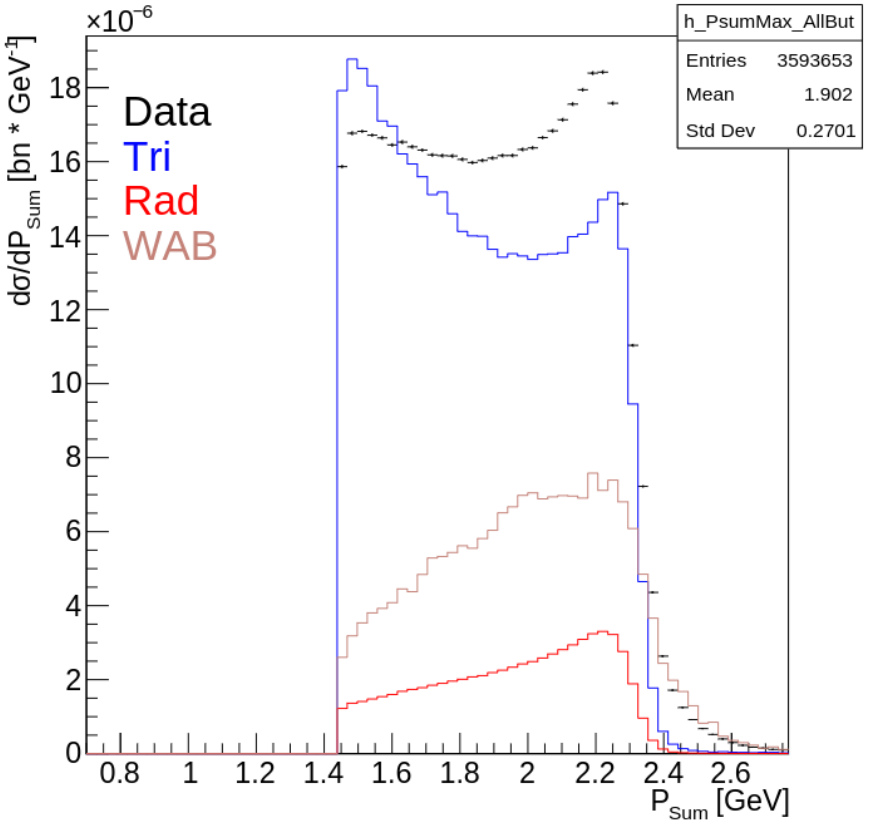

- Some events have multiple vertices that pass all cuts as a side-effect of complications in track formation.
  - One vertex is kept per event to avoid additional systematics.

Tracking Inefficiency and Track Killing

- There is a tracking inefficiency between data and Monte Carlo. To account for this, “track killing” is performed.
  - 5-hit tracks are tested against the track killing criteria and either retained or excluded.
  - 6-hit tracks are always retained.
- Track killing improves the discrepancy to around 9% – 11%.
  - The remaining inefficiency is expected due to >20% target thickness uncertainty and form factor knowledge uncertainty of a few percent.
  - This is not important as long as the discrepancy is not dependent on kinematics.

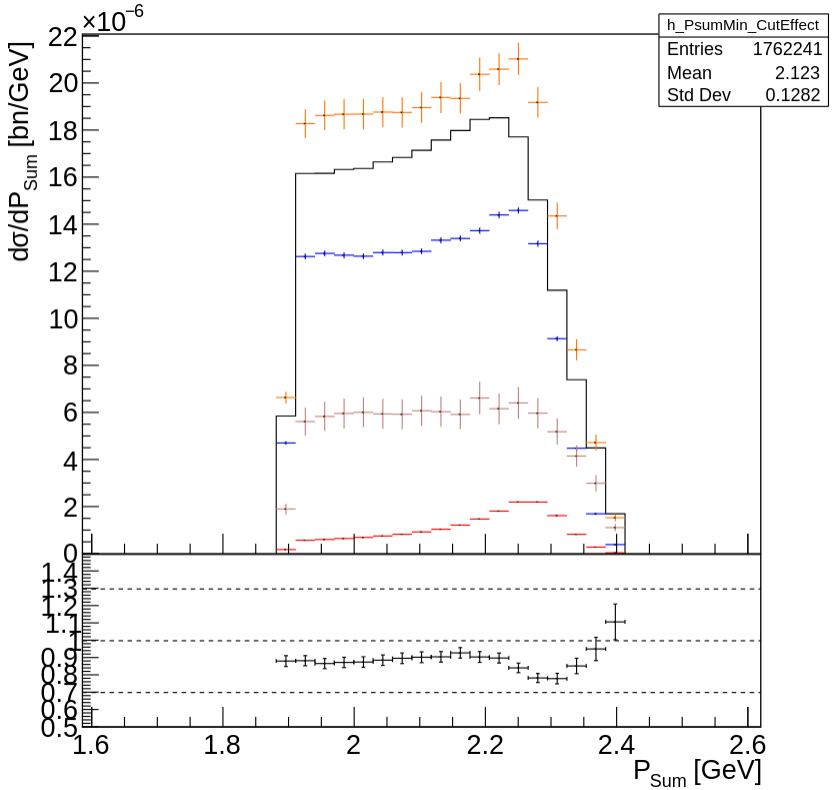

Cut Efficiencies Summary

- All cuts exclude a similar percentage of events between data and MC.

Cut Variable	Data Set					
	Data		Tri-beam	Rad-beam	WAB-beam	Tri+WAB
	V_0 Count	Cut Fraction	Cut Fraction	Cut Fraction	Cut Fraction	Cut Fraction
Preselection	2.682×10^9	1	1	1	1	1
$p_{sum} < 2.4$ GeV	9.015×10^6	0.9650	0.9933	0.9894	0.9232	0.9691
$p_{sum} > 1.9$ GeV	2.540×10^7	0.3425	0.2833	0.6436	0.5537	0.3375
$\lvert\Delta t_{cluster}\rvert < 1.43$ ns	8.951×10^6	0.9720	0.9932	0.9898	0.9928	0.9931
Single V_0	8.700×10^6	0.8602	0.9165	0.9280	0.8935	0.9084

Final Invariant Mass Distribution

- The final invariant mass distribution, after all vertex selection cuts are applied, is shown.